AIAA 2000-1956

Three-Dimensional Nacelle Aeroacoustics Code With Application to Impedance Eduction

Willie R. Watson
NASA Langley Research Center
Hampton, VA

6th AIAA/CEAS
Aeroacoustics Conference
June 12-14, 2000
Lahaina Hawaii, USA

THREE-DIMENSIONAL NACELLE AEROACOUSTICS CODE WITH APPLICATION TO IMPEDANCE EDUCTION

Willie R. Watson *
NASA Langley Research Center
Hampton, VA

Abstract

A three-dimensional nacelle acoustics code that accounts for uniform mean flow and variable surface impedance liners is developed. The code is linked to a commercial version of the NASA-developed General Purpose Solver (for solution of linear systems of equations) in order to obtain the capability to study high frequency waves that may require millions of grid points for resolution. Detailed, single-processor statistics for the performance of the solver in rigid- and soft-wall ducts are presented. Over the range of frequencies of current interest in nacelle liner research, noise attenuation levels predicted from the code were in excellent agreement with those predicted from mode theory. The equation solver is memory efficient, requiring only a small fraction of the memory available on modern computers. As an application, the code is combined with an optimization algorithm and used to educe the impedance spectrum of a ceramic liner. The primary problem with using the code to perform optimization studies at frequencies above 11kHz is the excessive CPU time (a major portion of which is matrix assembly). The research recommends that research be directed toward development of a rapid sparse assembler and exploitation of the multiprocessor capability of the solver to further reduce CPU time.

Nomenclature

$[A_I], [B_I], [C_I]$	major blocks
$[A(\zeta)]$	coefficient matrix
$[A_e]$	local element matrix
$[a_I], [b_I], [c_I]$	minor blocks matrix
c_0	ambient sound speed
dx, dy, dz	x, y and z differentials
$[D]$	diagonal matrix
$E(x, y, z)$	error function
f	source frequency
$\{F\}$	vector of source effects
W, H, L	width, height, and length of duct
w, h, l	width, height, and length of element
i	$\sqrt{-1}$
k	$2\pi f / c_0$, free-space wave number
M_0	u_0/c_0, mean flow Mach number
N, M, Q	total number of spanwise, transverse, and axial nodes
$N_I(x, y, z)$	three-dimensional basis
n	outward unit normal
$[L]$	lower triangular matrix
$p(x, y, z)$	acoustic pressure field
P_I	unknown node coefficients
$p_s(x, y)$	source pressure
R	liner resistance
Re{ }	real part of complex expression
u_0	uniform flow speed
$u(x, y, z)$	axial acoustic velocity
x, y, z	Cartesian coordinates
$[U]$	upper triangular matrix
$\{Z\}$	intermediate vector
ΔdB	noise attenuation level
ζ	$r + I\xi$, wall impedance
ζ_{exit}	exit impedance
ξ	liner reactance
ρ_0	ambient density
$\phi(z)$	axial acoustic power
$\{\Phi\}$	global vector of unknowns
$\{\Phi_e\}$	local vector of element unknowns
Subscripts:	
e	element number
I	basis function counter
J	minor blocks counter
s	source plane index
Superscripts:	
$IMAX$	number of unknown nodal coefficients
T	matrix transposition
$*$	complex conjugate

*Senior Research Scientist, Computational Modeling and Simulation Branch, Aerodynamics, Aerothermodynamics, and Acoustics Competency. Member of AIAA.

Introduction

Fan noise accounts for a significant portion of community noise radiated from both conventional and high bypass ratio engines. Noise reduction research today focuses on reducing the perceived noise levels of future aircraft by half relative to current levels within ten years. Installation of acoustic treatment (i.e., liners) into the nacelles of aircraft engines remains one of the most effective means for achieving these noise reduction goals.[1] However, future aircraft engines are being designed with higher bypass ratios, which have much shorter inlet ducts than conventional inlets. The shorter inlet duct associated with the higher bypass ratios has severely taxed the ability of conventional liners to absorb inlet noise effectively. To achieve the required noise reduction in the inlet for the higher bypass ratios, more advanced liners are needed. These include double- and triple-layer liners as well as those liners with variable surface impedances.[1] The acoustic treatment must be highly tuned (optimized) in order to provide sufficient noise reduction over the shorter length of the inlet duct.

To optimize the treatment for maximum sound suppression, fully three-dimensional nacelle aeroacoustic codes that account for the increased liner complexity and the mean flow are needed. Recent research in impedance eduction techniques has also highlighted the need for the development of three-dimensional codes to perform accurate impedance measurements in the presence of flow.[2] Currently, industry and government design codes treat only two dimensional nacelle designs. Although several approximate three-dimensional models are available,[3] these models make simplifying assumptions that are not generally valid for acoustic disturbances propagating within the walls of an aircraft nacelle.

Within an aircraft nacelle, the engine noise is often dominated by a few harmonics of a fundamental frequency. It is therefore convenient to use a frequency domain analysis in order to take full advantage of the presence of only a few harmonics in the acoustic field. The equations resulting from frequency domain analysis in aeroacoustics are indefinite and are generally solved by band solvers. However, when applied in three-dimensional computational methods, band solvers require excessive amount of central processing unit (CPU) time and memory (RAM). This requirement has limited nacelle aeroacoustic codes to the study of low frequency sound sources through axisymmetric nacelles.

The purpose of this work is to develop a fully three-dimensional code for nacelle aeroacoustics. First, the frequency domain differential equation and boundary conditions in the presence of flow are presented. The solution for the acoustic field is then approximated by a conventional finite element method. The finite element method leads to a large, sparse, linear system of equations. A commercial version of the NASA-developed General-Purpose Solver (GPS) is applied to reduce the CPU time and RAM required to obtain three-dimensional solutions. Several insights concerning the efficiency of the solver are revealed via numerical experimentation. Noise attenuation levels are compared to those predicted from mode theory for the range of frequencies of current interest in liner research. As an application, the three-dimensional model is used to educe the impedance of a ceramic liner for frequencies ranging from 4kHz to 11kHz.

Governing Equations and Boundary Conditions

Figure 1 is a sketch of the three-dimensional rectangular duct geometry used in this study. For the sake of simplicity, the mean flow in the duct is considered to have only a uniform subsonic axial component, that flows subsonically at a uniform speed, u_0, as shown. The computational volume enclosed by the duct is W units in width, H units in height and L units in length. At the source and exit boundary of the domain, respectively, the source plane pressure p_s and the exit plane impedance ζ_{exit} are known. In addition, the walls of the duct are lined with a sound-absorbing material whose impedance is denoted by ζ. Note that the three critical acoustic parameters (p_s, ζ_{exit}, and ζ) are allowed to vary along their respective boundaries with position (see equations (2) and (3)).

The equations that describe the propagation of acoustic pressure disturbances within the duct depicted in fig. 1 are derived from the Navier-Stokes and energy equations, neglecting viscous and heat conducting effects. The justification for the neglect of viscosity and heat-conduction is that the passage of sound waves through a uniformly moving fluid is an isentropic process. The equations that will be the subject of this investigation result from two additional assumptions:

1. Nonlinear acoustic effects can be neglected.

2. The acoustic disturbance has reached a periodic steady state.

Under these assumptions the equations which describe the conservation of mass, momentum, and energy for the flowing fluid may be combined into a single, second order, partial differential equation which describes the propagation of acoustic pressure disturbances in the duct:[4]

$$(1 - M_0^2)\frac{\partial^2 p}{\partial z^2} + \frac{\partial^2 p}{\partial x^2} + \frac{\partial^2 p}{\partial y^2} - 2ikM_0\frac{\partial p}{\partial z} + k^2 p = 0 \quad (1)$$

Although not considered here, Eq. (1) may be generalized to include mean flows with gradients, or may be suitably transformed to cylindrical coordinates and used to study cylindrical duct geometries. The source and exit plane boundary conditions are[2]

$$p = p_s \quad (2)$$

$$\frac{\partial p(S)}{\partial z} = \frac{-ikp(S)}{[\zeta_{\text{exit}}(S) + M_0]} \quad (3)$$

where S denote the (x, y, z) location along the boundary surface. The wall impedance boundary condition is[5]

$$\frac{\partial p(S)}{\partial n} = ik\left[\frac{p(S)}{\zeta(S)}\right] + 2M_0\frac{\partial}{\partial z}\left[\frac{p(S)}{\zeta(S)}\right] + \frac{M_0^2}{ik}\frac{\partial^2}{\partial z^2}\left[\frac{p(S)}{\zeta(S)}\right] \quad (4)$$

where s denote position along the surface of the liner.

The Finite Element Method

The numerical method chosen to solve the governing equation (1) coupled with the boundary conditions (2)−(4) is the finite element method. Details of the implementation of the finite element method in three dimensions closely parallels that described in an earlier two-dimensional paper.[2] Only sufficient detail is presented here to highlight the major differences between the two- and three-dimensional formulations.

When applied to the current three-dimensional nacelle aeroacoustics problem, the finite element method may be interpreted as an approximation to the continuous acoustic field as an assemblage of rectangular prism elements as shown in Fig. 2. Here N, M and Q evenly spaced points are assumed in the spanwise, transverse, and axial directions, respectively. A typical rectangular prism element with spanwise, transverse, and axial dimension w, h and l is shown in Fig. 3. The rectangular prism element consists of eight local node numbers labeled 1, 2, ..., 8, respectively as shown in Fig. 3. The objective is to obtain the unknown acoustic pressures at the nodes of each of the $(N-1)(M-1)(Q-1)$ elements.

A conventional Galerkin finite element method is used to minimize the field error. The field error function is defined as

$$E(x, y, z) = (1 - M_0^2)\frac{\partial^2 p(x,y,z)}{\partial z^2} + \frac{\partial^2 p(x,y,z)}{\partial x^2} + \frac{\partial^2 p(x,y,z)}{\partial y^2} - 2ikM_0\frac{\partial p(x,y,z)}{\partial z} + k^2 p(x, y, z) \quad (5)$$

Within each element, the acoustic pressure field $p(x, y, z)$ is approximated by using a set of linearly independent basis functions, $N_I(x, y, z)$:

$$p(x, y, z) = \sum_{I=1}^{IMAX} N_I(x, y, z)p_I \quad (6)$$

Linear and cubic Hermite basis functions are used with and without flow, respectively. For a two-dimensional rectangular element, the functional forms of these basis functions are given in Ref. 6, and these functional forms are easily generalized to three space dimensions. The variable exit impedance ζ_{exit} and wall impedance ζ are represented in a similar manner along each boundary element. The impedance boundary conditions (3) and (4) are satisfied using a weak formulation, just as in Ref. 2.

The contribution to the minimization of the field error for each element is expressed in matrix form as

$$\int_0^l \int_0^h \int_0^w EN_I \, dx \, dy \, dz = [A_e]\{\Phi_e\} \quad (7)$$

Assembly of the global equations for the computational domain is a basic procedure in the finite element method. Appropriate shifting of rows and columns is all that is required to add the local element matrix $[A_e]$ directly into the global stiffness matrix. Assembly of the elements for the entire domain results in a matrix equation of the form

$$[A]\{\Phi\} = \{0\} \quad (8)$$

The source pressure boundary condition must be applied to the system of equations (8) before a solution can be obtained. To satisfy the noise-source boundary condition, all nodal values of the acoustic pressure at the source plane are simply set to the known value of source pressure, $p_s(x, y)$. The insertion of these source boundary conditions leads to a modified set of equations of the form

$$[A(\zeta)]\{\Phi\} = \{F\} \quad (9)$$

The global matrix $[A(\zeta)]$ generated by Galerkin's method is a complex indefinite matrix. The structure of the matrix $[A(\zeta)]$ is shown in Eq. (10) for the zero flow case

$$[A(\zeta)] = \begin{bmatrix} [A_1]^T & [B_2] & & & \\ [B_2]^T & [A_2] & [B_3] & & \\ & \ddots & \ddots & \ddots & \\ & & & [B_Q]^T & [A_Q] \end{bmatrix} \quad (10)$$

Note that in the absence of flow, $[A(\zeta)]$ is a square symmetric block-tridiagonal matrix. This global

matrix contains several major blocks, $[A_I]$ and $[B_I]$, as shown in Eq (10). Each major block is an $NMxNM$ block-tridiagonal matrix as shown in the Expression (11) below

$$\begin{bmatrix} [a_1] & [b_2] & & & \\ [c_2] & [a_2] & [b_3] & & \\ & \ddots & \ddots & \ddots & \\ & & [c_N] & [a_N] \end{bmatrix} \quad (11)$$

Each minor block $[a_J], [b_J],$ and $[c_J]$ is an MxM tridiagonal complex matrix. The order of $[A(\zeta)]$ is $NMQxNMQ$. When flow is present, the structure of the coefficient matrix $[A(\zeta)]$, is similar to that without flow. However, when flow is present, the coefficient matrix $[A(\zeta)]$ will not be symmetric and each minor blocks $[a_J], [b_J],$ and $[c_J]$ will be block tridiagonal.

Many practical considerations regarding storage and solution efficiency arise from the structure of $[A(\zeta)]$. In Ref. 2, the solution to the discrete system in two space dimensions was obtained by using a band solver. However, in three dimensions, the bandwidth of $[A(\zeta)]$ is considerably larger than its two-dimensional counterpart. Thus, the band solver severely taxed computer resources by requiring storage and arithmetic operations on the inner null bands of $[A(\zeta)]$. This paper will focus on the use of an efficient sparse solver that will minimize the "fill" within the inner null bands of $[A(\zeta)]$.

The Equation Solver

In this research effort, the Vector Sparse Solver[TM] (VSS) software[†],[7] (a commercial version of NASA's GPS[8] developed by Solversoft) was exercised to obtain the solution to the aeroacoustic system defined by Eq. (9). The GPS equation solver had its genesis in the solution to large aerospace structures in computational mechanics. It was subsequently extended to support matrices that are sparse or dense, indefinite, real or complex. In addition, Solversoft[TM] has extended VSS[TM] to solve nonsymmetric systems of equations often generated for example, in aeroacoustics problems containing mean flow. The method of solving used to obtain the solution to the aeroacoustic system defined by Eq. (9) was as follows:

1. Reorder the system of equations (Note that reordering of the equations reduces RAM and

CPU time by minimizing the "fill" within the inner null bands of the coefficient matrix.)

2. Factorize the reordered matrix as

$$[A] = [L][U] \quad (12)$$

A fairly general scheme exists for computing $[L]$ and $[U]$. When the matrix is symmetric (i.e., $M_0 = 0$), $[U]$ may be obtained from $[L]$ with negligible computational effort:

$$[U] = [D][L]^T \quad (13)$$

where $[D]$ is a diagonal matrix

3. Use a forward solution phase to obtain an intermediate vector $\{Z\}$:

$$[L]\{Z\} = \{F\} \quad (14)$$

4. The solution for the vector $\{\Phi\}$ is obtained by using backward substitution:

$$[U]\{\Phi\} = \{Z\} \quad (15)$$

The key innovation of the VSS software is that $[L]$ and $[U]$ are computed efficiently, with due attention given to eliminating computations with zero elements, while maintaining low storage and CPU time. A second innovation is a novel reordering method that retains the benefit of a multiple-minimum degree (MMD) reordering at a fraction of the MMD reordering time. This benefit is accomplished by reordering a subset of the equations. The solver software requires that only the nonzero coefficients in $A[(\zeta)]$ be stored in RAM. Further, the nonzero coefficients are stored in row format and as a single vector to facilitate the solution procedure. The VSS software exploits the matrix characteristics (real/complex, symmetric/nonsymmetric, in-core/out-of-core) of the application and also exploits the hardware features of the computing system. Only a small fraction of the capability of the solver was used in this research effort (i.e., only the complex, symmetric, in-core capability was required). The equation solver used in this work included several other recent innovations that are discussed in detail elsewhere.[8]

Results

An in-house computer code that assembles the coefficient matrix $[A(\zeta)]$ in the required solver format was combined with the VSS software in order to provide the capability to solve three-dimensional aeroacoustics problems. Three-dimensional solutions are

presented for both rigid- and soft-wall ducts in the absence of flow. Results were computed on an in-house SGI ORIGIN 2000^{TM} computer that contained slightly more than 12 gigabytes of RAM and eight processors. Computations presented in this paper were run on only a single processor with double-precision (64-bit) arithmetic. Computations are presented for a geometry identical to that of the Langley Flow Impedance Tube.[2] This three-dimensional duct has a square cross section 0.508 m in width ($W = H = 0.508$ m). The duct is .812 m in length (L=0.812 m) with the liner located on the lower wall. The upper and two side walls of the duct are rigid. A much more complete description of the duct is given in Ref. 2. All calculations were performed at standard atmospheric conditions and the source frequency was chosen to span the full range of frequencies that are currently of interest in duct liner research.

The left ordinate in Fig.4 shows a plot of the highest order mode cut on in the spanwise and transverse direction of the rigid-wall ($\zeta = \infty$) duct for frequencies of current interest in liner research. The right ordinate in the figure shows the order of the matrix $[A(\zeta)]$ needed to resolve all cut on modes in the three-dimensional duct. Here, the author used the general rule that approximately 12 points per wavelength is required in each of the three coordinate directions to accurately resolve a propagating (cut on) mode. Results are not shown for frequencies below 4kHz because only the plane wave mode was cut on in the duct. Source frequencies below 4kHz may be analyzed with a two-dimensional code such as that developed in an earlier paper.[2] Note that at the high frequency end of the spectrum (17kHz) in each coordinate direction, five modes are cut on in addition to the plane wave mode. A matrix order of slightly more than 434000 is required to accurately resolve all cut on modes that propagate at this frequency.

Figure 5 shows the CPU time and RAM required to solve for the acoustic field in the rigid-wall duct. The source was a plane wave source and the exit boundary condition was chosen so that the exit plane was reflection free ($\zeta_{\text{exit}} = 1$). The CPU times shown in the figure correspond to those required to obtain the solution vector $\{\Phi\}$ after matrix assembly. Generally, the CPU times required to perform the forward and backward solutions were less than 1% of that required to perform the $[L][U]$ factorization of the matrix. The CPU times required to obtain the solution range from 0.9 sec at 4kHz to a maximum of nearly three hr at 17kHz. The RAM range from a low of 4.4 megabytes at 4kHz to slightly more than 2.1 gigabytes at 14kHz. The RAM requirements are

not monotonic because there is more "fill" within the inner null bands of $[A(\zeta)]$ at 14kHz than 17kHz. Note that all solutions consumed only a fraction of the 12 gigabytes of RAM available on the SGI ORIGIN 2000^{TM}.

To check the accuracy of the solution vector, the author used the reduction in the sound power from the entrance to the exit of the duct (i.e., ΔdB) as a metric. This quantity is a physically more meaningful norm than the error norm of the computed solution because it is the quantity perceived by the human ear as the noise source propagates down the duct. This metric has units of decibels and is defined as

$$\Delta dB = 10 \log_{10} \frac{(1/2)\text{Re}\{\phi(0)\}}{(1/2)\text{Re}\{\phi(L)\}} \qquad (16)$$

$$\phi(z) = \int_0^W \int_0^H \{p(x,y,z)u^*(x,y,z)\}dxdy \qquad (17)$$

For the zero flow calculations considered here, the acoustic velocity is related to the pressure gradient via the axial momentum equation:

$$u(x,y,z) = \frac{-1}{(2i\rho_0 \pi f c_0)} \frac{\partial p(x,y,z)}{\partial z} \qquad (18)$$

An exact mode solution shows that no sound is attenuated in the rigid-wall duct (i.e., $\Delta dB = 0$). The solution vector $\{\Phi\}$, obtained from the equation solver was used to numerically compute the noise attenuation level, ΔdB. The attenuation levels computed from the VSS solution vector in the rigid wall duct, were in excellent agreement with the exact mode solution of zero. Figure 6 shows a plot of the VSS solution time and the sparse matrix assembly time in the rigid wall duct. Note that at the high frequency end of the spectrum, sparse matrix assembly time is approximately twice that required to obtain the VSS solution.

Statistics have also been computed for a ceramic liner with the resistance (R) and reactance (ξ) spectrum shown in Fig. 7. At each frequency, the sound source was chosen as the highest order cut on mode in the duct and the exit impedance was chosen to eliminate reflections from the duct exit. Soft wall results in this paper have been purposely restricted to this range of parameters because approximate modal solutions are available to check the solver solution for the noise attenuation levels. The CPU and RAM statistics for the soft-wall duct were nearly identical to those of the rigid-wall duct. Figure 8 compares the noise attenuation levels over the ceramic liner to those of mode theory. Noise attenuation levels

predicted with the model are in excellent agreement with mode theory.

In a recent paper[2] a numerical method for extracting the impedance of an acoustic material located in a two-dimensional duct was developed and validated. The impedance extraction method required input of the source pressure p_s, exit impedance ζ_{exit}, and upper wall pressure. The three-dimensional model described here has been linked to this impedance extraction technique in order to provide the capability to extract impedances in three-dimensional sound fields. Because measured three-dimensional data was not available, the boundary data required to educe the impedance was synthesized from the analytical mode solution. Figure 9 compares the resistance and reactance educed by using the current model to the known values for frequencies of 4kHz, 7kHz, and 11kHz. Excellent comparisons were obtained between the known and educed resistance and reactance values. Impedance eductions for frequencies above 11kHz were not performed because the CPU times (a significant part is matrix assembly) to educe the impedances became excessive.

Concluding Remarks

A three-dimensional nacelle acoustic code to account for uniform mean flow and variable surface impedance liners has been developed. The code was linked to a commercial version of the NASA-developed General Purpose Solver to obtain the capability to study high frequency sound waves that may require millions of grid points for resolution. Over the range of frequencies of current interest in nacelle liner research, noise attenuation levels predicted from the code were in excellent agreement with those predicted from mode theory. The equation solver is RAM efficient, requiring only a small fraction of the RAM available on a modern computer such as the SGI ORIGIN 2000^{TM} used in this study. The code is tractable for optimization studies with source frequencies up to 11kHz. The problem with using the code to perform optimization studies at frequencies above 11kHz is the excessive CPU time (a major portion of which is matrix assembly time). This research therefore recommends that research be directed toward development of a rapid sparse assembler and that the multiprocessor capability of the solver be exploited to further reduce CPU time so that optimization studies become tractable for frequencies above 11kHz.

References

1. Bielak, et al., "Development of Technical Knowledge and Design Concepts for Advanced Turbofan Duct Acoustic Linings," NASA Contract Interim Report, Contract Number NAS1-97040, Dec, 1997.

2. Watson, Willie R., Jones, M. G., and Parrott, T. L., "Validation of an Impedance Eduction Method in Flow," *AIAA Journal*, Vol. 37, No. 7, 1999, pp. 85--94.

3. Dougherty, R. P., "A Wave-Splitting Technique for Nacelle Acoustic Propagation," Proceedings of the 3rd AIAA/CEAS Aeroacoustic Conference, 1997, pp.550−556.

4. Kraft, R. E., "Theory and Measurements of Acoustic Wave Propagation in Multi-Segmented Rectangular Ducts," Ph.D. Thesis, University of Cincinnati, 1976.

5. Myers, M. K., "On the Acoustic Boundary Condition in the Presence Of Flow," *Journal Of Sound And Vibration*, Vol. 71, No. 3, 1980, pp. 429−434.

6. Chandrakant, S., and Abel, John F., *Introduction to the Finite Element Method*, Van Nostrand Reinhold, New York, 1972.

7. Baddourah, M., "Solution of Matrix Equations Using Sparse Techniques," in: *The Role of Computers in Research and Development at Langley Research Center*, NASA CP-10159, Oct. 1994, pp. 130−146.

8. Storaasli, O. O., "Performance of NASA Equation Solvers on Computational Mechanics Applications," *Proceedings of the 37th AIAA/ASME/ASCE/ANS/ASC Structures, Structural Dynamics and Materials Conference*, Salt Lake City, 1996, pp. 1680−1685.
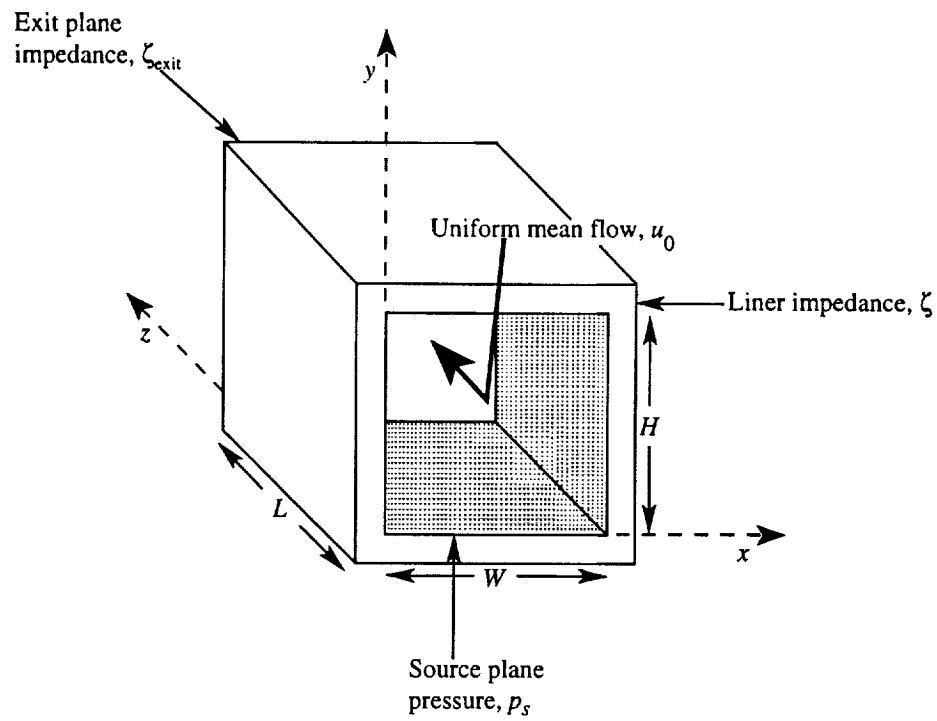
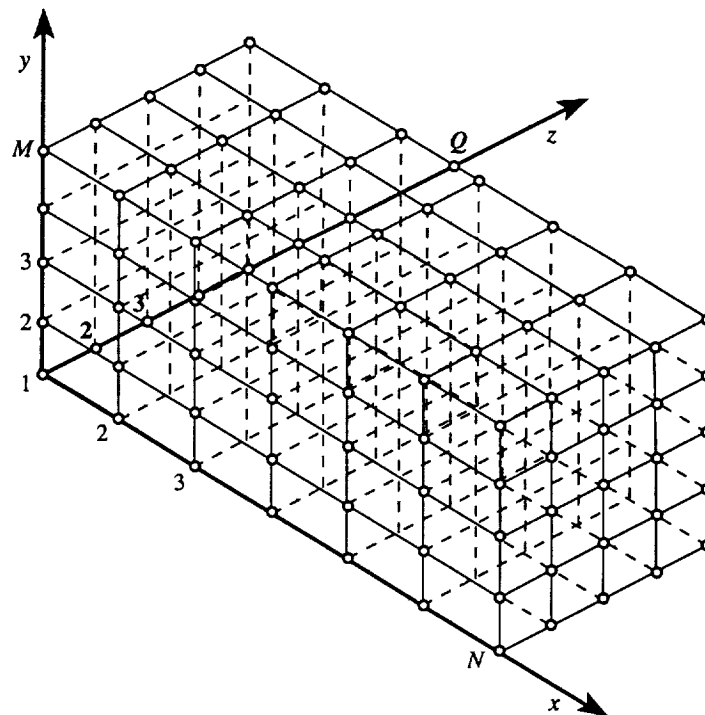Fig. 1   Schematic of three-dimensional duct and coordinate system.

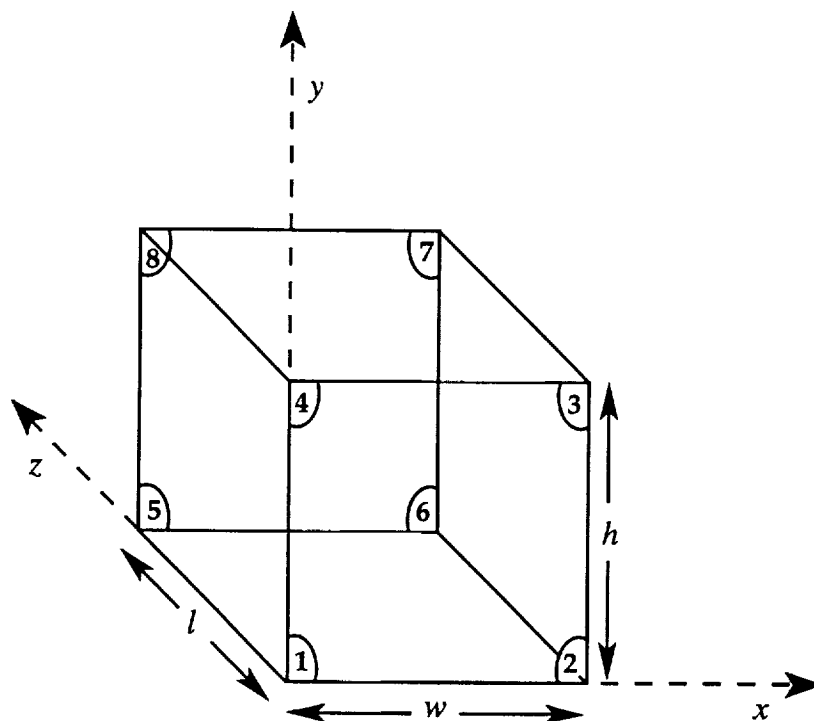Fig. 2   Finite-element discretization of computational volume.

Fig. 3 Three-dimensional finite element and coordinate system.
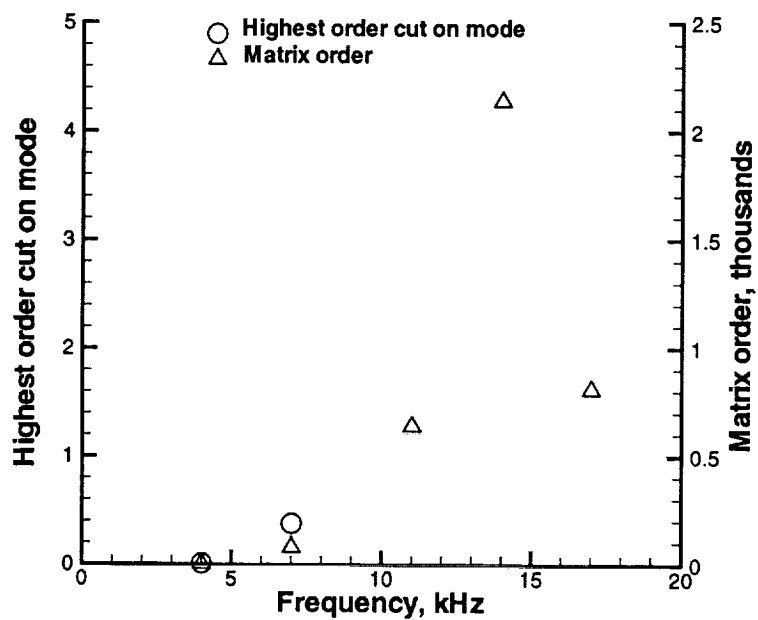

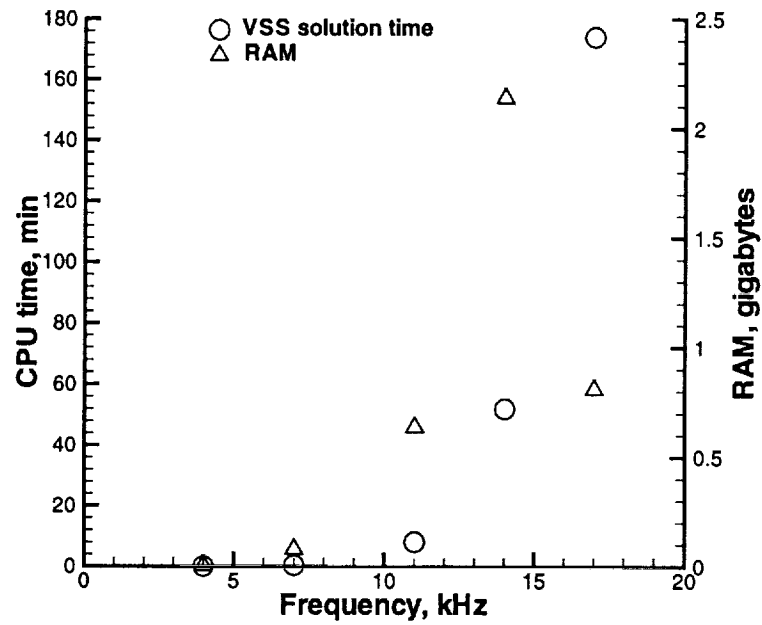Fig. 4 Highest order cut on modes in a three-dimensional rigid-wall duct.

Fig. 5   CPU time and RAM statistics for a three-dimensional rigid-wall duct.
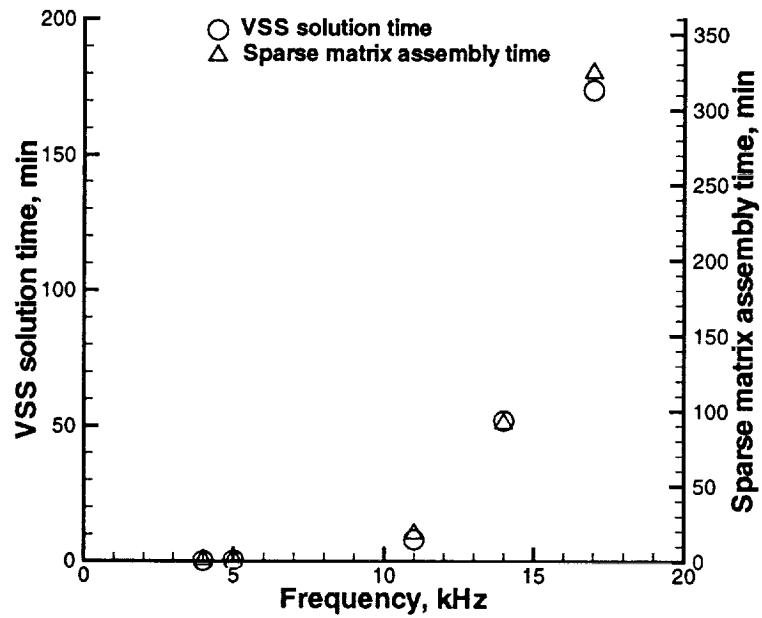

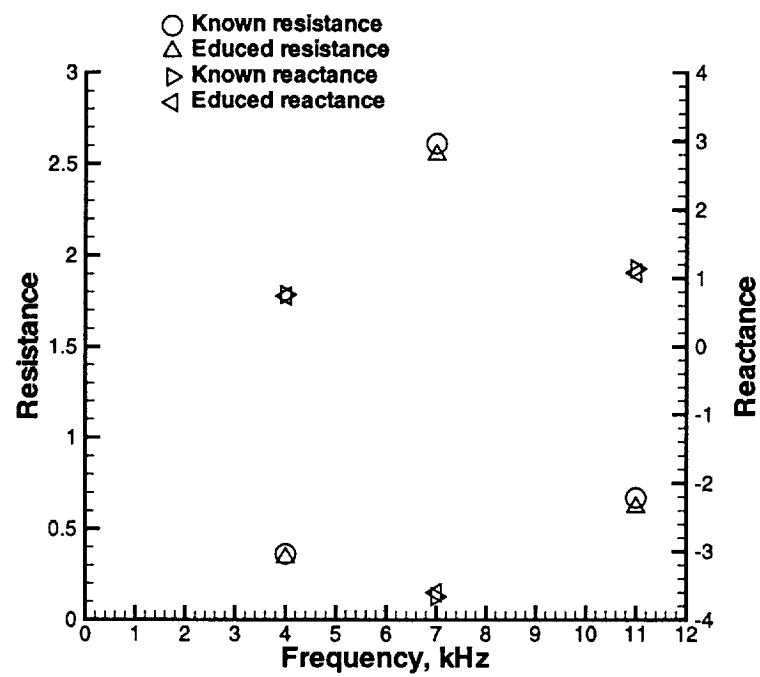Fig. 6   VSS solution and sparse matrix assembly times in a rigid-wall duct.

Fig. 9   Educed impedance of the ceramic liner in a three dimensional duct.